

Investigating the monotonic behaviour of hybrid tripod suction bucket foundations for offshore wind towers in sand

Faizi, Koohyar; Faramarzi, Asaad; Dirar, Samir; Chapman, David

DOI:

[10.1016/j.apor.2019.05.018](https://doi.org/10.1016/j.apor.2019.05.018)

License:

Creative Commons: Attribution-NonCommercial-NoDerivs (CC BY-NC-ND)

Document Version

Peer reviewed version

Citation for published version (Harvard):

Faizi, K, Faramarzi, A, Dirar, S & Chapman, D 2019, 'Investigating the monotonic behaviour of hybrid tripod suction bucket foundations for offshore wind towers in sand', *Applied Ocean Research*, vol. 89, pp. 176-187. <https://doi.org/10.1016/j.apor.2019.05.018>

[Link to publication on Research at Birmingham portal](#)

Publisher Rights Statement:

Checked for eligibility: 26/07/2019

General rights

Unless a licence is specified above, all rights (including copyright and moral rights) in this document are retained by the authors and/or the copyright holders. The express permission of the copyright holder must be obtained for any use of this material other than for purposes permitted by law.

- Users may freely distribute the URL that is used to identify this publication.
- Users may download and/or print one copy of the publication from the University of Birmingham research portal for the purpose of private study or non-commercial research.
- User may use extracts from the document in line with the concept of 'fair dealing' under the Copyright, Designs and Patents Act 1988 (?)
- Users may not further distribute the material nor use it for the purposes of commercial gain.

Where a licence is displayed above, please note the terms and conditions of the licence govern your use of this document.

When citing, please reference the published version.

Take down policy

While the University of Birmingham exercises care and attention in making items available there are rare occasions when an item has been uploaded in error or has been deemed to be commercially or otherwise sensitive.

If you believe that this is the case for this document, please contact UBIRA@lists.bham.ac.uk providing details and we will remove access to the work immediately and investigate.

1 **Investigating the Monotonic Behaviour of Hybrid Tripod Suction Bucket**

2 **Foundations for Offshore Wind Towers in Sand**

3 Koohyar Faizi¹, Asaad Faramarzi², Samir Dirar³, David Chapman⁴

4

5 ¹PhD student, School of Engineering, University of Birmingham, Edgbaston,

6 Birmingham B15 2TT, UK, K.Faizi@pgr.bham.ac.uk

7 ²Assistant Professor, School of Engineering, University of Birmingham,

8 Edgbaston, Birmingham B15 2TT, UK, A.Faramarzi@bham.ac.uk

9 ³Associate Professor, School of Engineering, University of Birmingham,

10 Edgbaston, Birmingham B15 2TT, UK, S.M.O.H.Dirar@bham.ac.uk

11 ⁴Professor, School of Engineering, University of Birmingham, Edgbaston,

12 Birmingham B15 2TT, UK, d.n.chapman@bham.ac.uk

13

14

15 **Abstract:** Existing tripod suction bucket foundations, utilised for offshore wind
16 turbines, are required to resist significant lateral loads and overturning moments
17 generated by wind and currents. This paper presents an innovative type of tripod bucket
18 foundation, ‘hybrid tripod bucket foundation’, for foundations of offshore wind
19 turbines, which has the ability to provide a larger overturning capacity compared with
20 conventional tripod buckets. The proposed foundation consists of a conventional tripod
21 bucket combined with three large circular mats attached to each bucket. A series of
22 experiments were conducted on small-scale models of the proposed foundation
23 subjected to overturning moment under 1g conditions in loose sand. Different circular
24 mat diameter sizes with various bucket spacings were considered and the results were
25 compared with conventional tripod bucket foundation. Finite element models of the
26 proposed foundation were developed and validated using experimental results and were
27 used to conduct a parametric study to understand the behaviour of the hybrid tripod
28 bucket foundation. The results showed that there is a significant increase in overturning
29 capacity provided by the novel foundation. The results of this work can significantly
30 improve lowering the costs associated with installation of foundations to support
31 offshore wind turbines.

32 **Keywords:** Overturning capacity; Hybrid tripod bucket foundations; Sand; Finite
33 element models

34

35 **1. Introduction**

36 Large horizontal and overturning bearing capacities are generally the
37 key design requirements for offshore shallow foundations [1].

38 Suction bucket foundations (monopod bucket), also known as a skirted shallow
39 foundations [2], have recently been considered for offshore wind turbines (OWTs) as a
40 cost effective alternative to conventional foundations [3]. As future generations of
41 offshore wind turbines are likely to have taller towers and be located further away from

42 the coast, the standard monopod foundations may become uneconomic and tripod
43 suction buckets may be more suitable [4].

44 Tripod bucket foundations are a standard three-legged structure made of cylindrical
45 bucket foundations. The central steel shaft of the tripod is attached to the turbine tower
46 by tubular space frames. This type of foundation is a popular design due to the smaller
47 diameter buckets, which reduces the probability of structural failure and easier
48 installation, [5] and provides higher bearing capacity for the foundations of OWTs
49 compared with single leg foundations [6, 7].

50 In case of single bucket foundation, as used in OWTs, the most unfavourable loading
51 condition is large overturning moments due to its low embedment depth [8]. A
52 large penetration to diameter ratio (>1) of the bucket typically has been
53 recommended to obtain satisfactory overturning capacities [9]. Using large buckets is
54 another way to increase capacities. However, as suction buckets are sensitive to
55 structural buckling during the installation process due to the profile characteristics
56 (thin-walled structures) [10, 11], installation of a very large thin wall bucket involves
57 significant risks of buckling. A large diameter suction bucket therefore requires a
58 significant number of stiffeners to prevent skirt buckling during installation. However,
59 any additional stiffeners may adversely impact the installation process [12].

60 Apart from the shape, the load transfer mechanism from the foundation to the soil is the
61 main difference between the mono and tripod bucket foundations [7]. The large
62 overturning moment can be resisted by a combination of tension and compression on
63 the windward and leeward legs in a tripod foundation, while a single bucket only
64 transfers the loading moment by the individual bucket surface interfaces with
65 surrounding soil [2, 13]. The installation process of the tripod bucket foundation into
66 the seabed is similar to that of the single suction bucket foundation (monopod). After
67 an initial penetration of the bucket into the seabed caused by self-weight, further
68 penetration is achieved by pumping air and water out of the bucket [14-17].

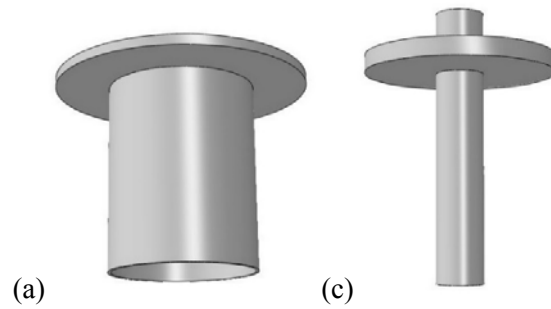
69 The bearing capacity of the single suction bucket foundations has been extensively
70 studied in different soil types [15, 18-20], whereas only a few studies have examined
71 the behaviour of tripod suction bucket foundations under lateral loading [21-23].
72 Various bucket and soil parameters have a direct influence on the bearing capacity of
73 the tripod bucket foundation, such as the ratio of the bucket spacing to the bucket
74 diameter (S/D), the embedment depth of the bucket (L), the soil–bucket friction angle
75 (δ) and the unit weight (γ) of the soil [21, 24, 25].

76 Although the increased capacity of tripod buckets has been demonstrated by increasing
77 the spacing of the buckets [22, 24], this will impose significant additional costs to the
78 structure of the space frames, thereby reducing the cost-effectiveness of tripod
79 foundations. This paper proposes a novel tripod foundation taking advantage of
80 combining tripods with circular mats as additional supporting structural elements.
81 Hereafter, this is referred to as a hybrid tripod bucket foundation. The hybrid tripod
82 bucket foundation aims to provide additional horizontal and moment capacity by
83 optimising the bucket spacing and consequently minimise the construction and
84 installation costs associated with large diameter skirted foundations.

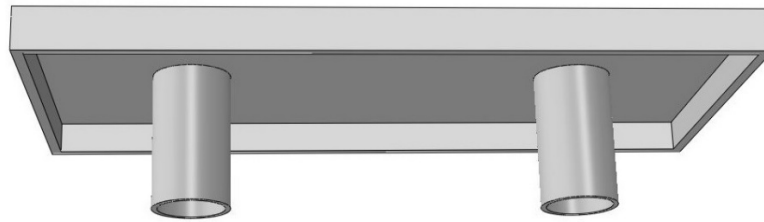
85 The hybrid foundation concept has been considered in past studies for OWTs, for
86 example these can be a combination of single suction buckets (Fig. 1a), multiple suction
87 buckets [26-28] (Fig. 1b) or mono-pile foundations (Fig. 1c) [29, 30] fitted on a mat
88 foundation, in which the mat contributes to enhancing the load capacity. A hybrid
89 single bucket foundation, which is a combination of a circular mat and a suction bucket,
90 was shown to provide a higher bearing capacity compared to a conventional caisson in a
91 study by [31]. However, the combination of a circular mat foundation and a
92 conventional tripod bucket foundation to improve the overturning capacity has not been
93 considered previously.

94 This study aimed to investigate the influence of including large mats to the tripod
95 suction bucket in loose sand subjected to horizontal loading by means of numerical and
96 experimental modelling.

97



98



99

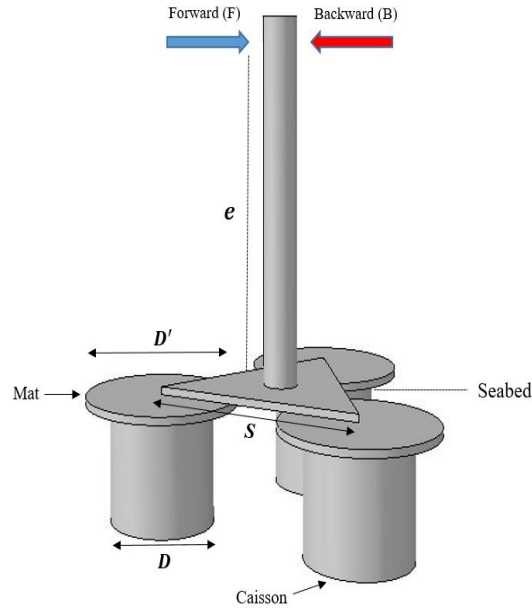
(b)

100 **Fig. 1.** Some proposed hybrid foundations concepts from previous research studies, (a) a
101 modified suction bucket, (b) a skirted mat with suction buckets, (c) a hybrid mono-pile
102 foundation.

103

104 **2. Methodology**

105 The proposed hybrid foundation consists of three single bucket foundations combined
106 with three large circular mats attached to each bucket foundation. The general concept
107 is shown in Fig. 2. In the conventional tripod bucket foundation, the bearing capacity is
108 provided by three rigidly connected bucket foundations, while in this proposed hybrid
109 foundation, the resistance is offered by a combination of the buckets and the circular
110 mats. In the proposed hybrid foundation the circular mats are in complete contact with
111 the soil surface providing greater resistance against the overturning moments.



112

113 **Fig. 2.** Schematic of the hybrid three suction bucket and mat foundation. The key dimensions
 114 and loading condition are also shown

115

116 The experiments were conducted at small-scale under 1-g condition. Different
 117 bucket spacing (S) and loading directions (backward and forward) were evaluated on
 118 the basis of overturning resistance of the conventional and hybrid tripod bucket
 119 foundations. In particular, forward and backward titles are given to the models with
 120 respect to the loading direction, i.e. backward used where the loading direction is
 121 towards a single bucket of a tripod foundation and the other two buckets are being
 122 rotated out of the seabed (Fig. 2).

123 Numerical analyses were conducted of the experiments for both the conventional and
 124 hybrid tripod bucket models using the finite-element (FE) method software, ABAQUS.
 125 The results of the experiments have been used to develop and validate FE models of the
 126 proposed system in order to understand the behaviour and the mechanisms in which the
 127 proposed hybrid system in a tripod foundation contribute to resistance against
 128 overturning moment. The effect of the circular mat diameter was also investigated using
 129 the validated FE model on the overturning resistance of the hybrid tripod bucket
 130 foundation.

131

132

133 3. Experimental Procedure

134 3.1 Materials and model preparation

135 The prototype was scaled down to 1/100, and a bucket embedment depth ratio (L/D) of
136 1 and a skirt width to bucket diameter ratio (t/D) = 0.02, were considered. The distance
137 between the buckets is expressed by the spacing ratio S/D , where S is the axial distance
138 between the circular buckets and D is their diameter (Fig.1). Experiments were
139 performed using various normalised spacings, S/D , ranging from 1.13 to 3.13.

140 The three conventional buckets with the external diameter (D) and embedment depth
141 (L) of 75 mm were connected with an adjustable plate. The caisson specimens
142 were fabricated from a smooth stainless steel tube with a wall thickness (t) of 1.2 mm.
143 The adjustable mechanism consisted of an equilateral triangular plastic plate (200 mm
144 long and 5 mm thick) with three linear holes in each angle. The three buckets were
145 connected to the adjustable mechanism by screws. By adjusting the distance between
146 the buckets, three different configurations could be created (more details are provided
147 in section 5.2). Three circular mats with a diameter of 120 mm, made of plastic, were
148 used to replace the conventional suction bucket caps and help to create the hybrid tripod
149 foundation (Fig. 3).



150

151 **Fig. 3.** Hybrid foundation model used in the experiments, with $D' = 120 \text{ mm}$ and $S = 165 \text{ mm}$

152

153 The horizontal load was applied to an extension rod (tower with 230 mm tall) that was
154 rigidly connected to the top of the centre of the base (triangular plate). Reinforcement
155 bracing between the top cap and the tower in the prototype were omitted in the model
156 for simplification. The circular mats and the towers made of plastic to reduce the effects
157 of additional weight affecting the bearing capacity.

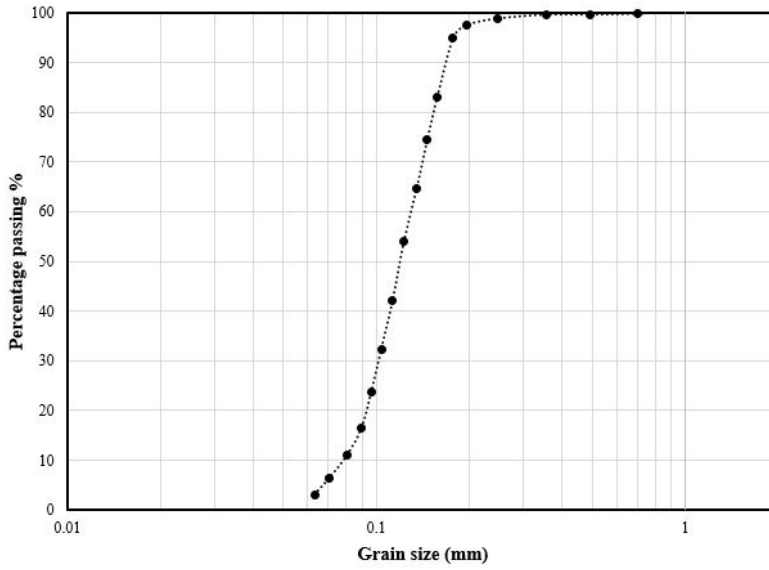
158 Tests were conducted in a strong cylindrical container. The container had an inner
159 diameter of 550mm, with a thickness of 30mm and a height of 600mm, and was filled
160 with dry Redhill 110 silica sand. The particle size distribution of the Redhill 110 silica
161 sand is shown in Fig. 4. A 100 mm thick layer of gravel was placed uniformly at the
162 base of the tank to provide a stiff layer underneath the sand layer. The sand layer was
163 prepared using a pluviation method to achieve the targeted density ($D_r = 23\%$). The
164 model buckets were installed in the dry sand by pushing rather than by suction. The
165 pushing process was carried out very gently to avoid any major disruption to the soil
166 density. Previous studies showed that the effect of the installation technique on the
167 subsequent behaviour of a single bucket is negligible [32].

168 The models were installed into the soil at a rate of 0.1 mm/s until the lid made complete
169 contact with the top of the sand. **The tests were carried out under drained soil conditions
170 to explore the drained response of the model foundation with a loading rate of 0.1mm/s.**

171 The properties of the Redhill 110 silica sand used in this study (Table 1) were obtained
172 from the study conducted by Kelly et al.[33] and Villalobos et al. [34, 35].

173

174



175

Fig. 4. Particle size distribution curves for Redhill 110

176

177

178

Table 1. Physical properties of sand used in the model tests, Redhill 110

| Properties | Value |
|--|------------------------|
| $d_{10}, d_{30}, d_{50}, d_{60}$ (mm) | 0.08, 0.10, 0.12, 0.13 |
| Coefficients of uniformity, C_u and curvature C_c | 1.63, 0.96 |
| Specific gravity, G_s | 2.65 |
| Minimum dry density, γ_{min} (kN/m ³) | 12.76 |
| Maximum dry density, γ_{max} (kN/m ³) | 16.80 |
| Angle of friction of the soil, ϕ | 36° |
| Permeability (m/s) | 3.8×10^{-4} |

179

180

181

3.2 Test procedure

182

For all the models, to create a moment, M , a horizontal load H' was applied using an

183

electric actuator at a certain height (230 mm) above the cap of the tripod bucket. An

184

eccentricity ratio (i.e. $M/(H'D)$) equal to 2.9 was used in this study, which corresponds

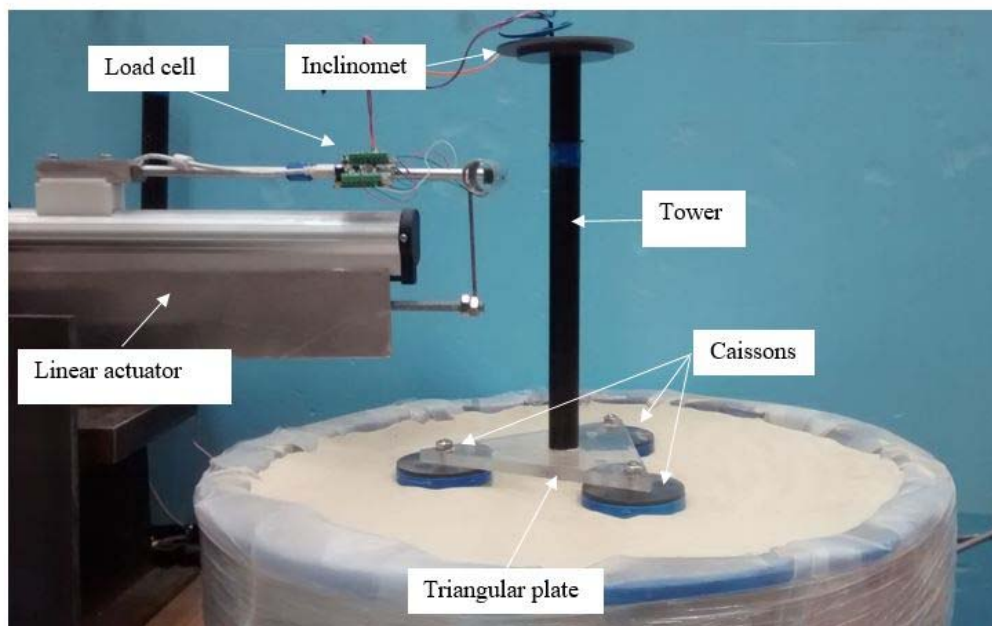
185

to tall wind turbine towers (>100 m). A load cell was attached to the actuator to

186 measure the applied force. The rotation of the foundation was recorded using an
187 inclinometer sensor placed on the top of the tower (as shown in Fig. 5).

188 Fig. 5(b) shows the plan view of the experimental set up and the loading system. As
189 illustrated, the model tripod foundations were placed in the middle of the model
190 container. The model tests were carried out in the central part of the container to ensure
191 minimal influence due to the wall boundary conditions.

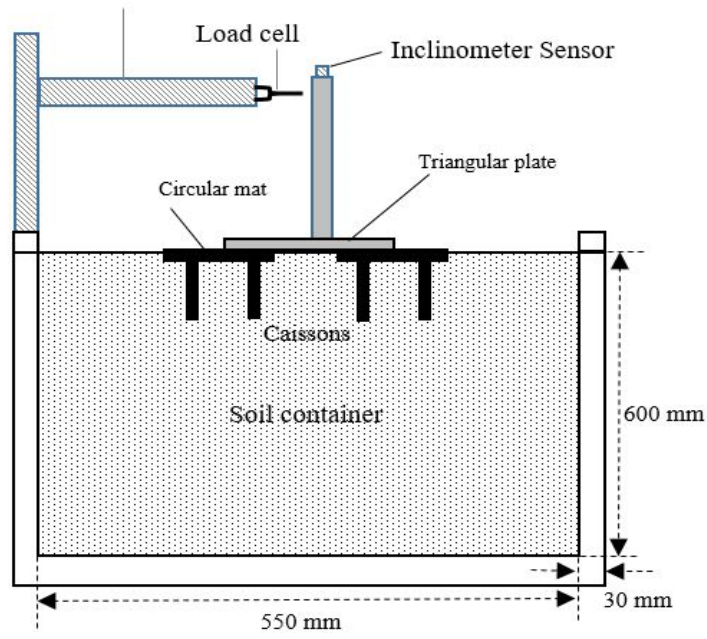
192 All the information related to the models and tests are summarised in Table 2; in this
193 table the conventional tripod bucket foundations and the hybrid tripod bucket
194 foundations are denoted C and H, respectively. The results from the experiments are
195 presented in section 5, where they have been used to validate the results of the
196 numerical models.



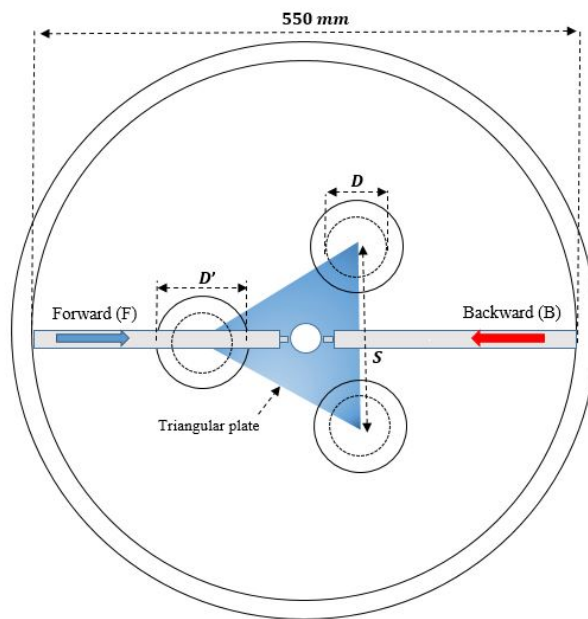
197

198 (a)

Linear actuator (Horizontal load)



199
200 (b)
201



202
203 (c)

204
205 **Fig. 5.** Testing system with loading actuator and tripod model (a) overview of the experimental
206 setup; (b) schematic of elevation view; (c) schematic of setup plan view

207

Table 2. Summary of the physical tests and numerical model analyses

| Test ID | S (mm) | Forward (F)/ Backward (B) ** | Caisson (D) and Circular mat (D') diameters (mm) | EXP/FEM*** |
|---------|----------|---------------------------------|--|------------|
| C1* | 95 | F | $D = 75$ | EXP/FEM |
| C2* | 95 | B | $D = 75$ | EXP/FEM |
| C3* | 130 | F | $D = 75$ | EXP/FEM |
| C4* | 130 | B | $D = 75$ | EXP/FEM |
| C5* | 165 | F | $D = 75$ | EXP/FEM |
| C6* | 165 | B | $D = 75$ | EXP/FEM |
| C7 | 200 | F | $D = 75$ | FEM |
| C8 | 200 | B | $D = 75$ | FEM |
| C9 | 235 | F | $D = 75$ | FEM |
| C10 | 235 | B | $D = 75$ | FEM |
| H1* | 130 | F | $D' = 120$ | EXP/FEM |
| H2* | 130 | B | $D' = 120$ | EXP/FEM |
| H3* | 165 | F | $D' = 120$ | EXP/FEM |
| H4* | 165 | B | $D' = 120$ | EXP/FEM |
| H5 | 200 | F | $D' = 120$ | FEM |
| H6 | 200 | B | $D' = 120$ | FEM |
| H7 | 235 | F | $D' = 120$ | FEM |
| H8 | 235 | B | $D' = 120$ | FEM |
| H9 | 235 | F | $D' = 120$ | FEM |
| H10 | 235 | B | $D' = 120$ | FEM |
| H11 | 235 | F | $D' = 142.5$ | FEM |
| H12 | 235 | B | $D' = 142.5$ | FEM |
| H13 | 235 | F | $D' = 180$ | FEM |
| H14 | 235 | B | $D' = 180$ | FEM |

*Reference tests

**F=Forward

B=Backward

*** EXP= Experiment

FEM= Finite element method

210

211 4. Numerical Simulation

212 To estimate the bearing capacity of the hybrid tripod bucket foundations in **drained**

213 sandy soils, three-dimensional (3D) finite element (FE) models were developed using

214 the commercial software ABAQUS; to reduce the computation time, only a half of the

215 foundation and the ground were modelled taking advantage of the symmetry within the
216 problem.

217 FE analysis was adopted to model the 3D geometry of the conventional and
218 hybrid tripod bucket foundations, and the appropriate soil–foundation interaction. Figs.
219 6a and 6b show a schematic of the conventional and hybrid tripod bucket foundation
220 problem in the FE model, respectively. To model the sand behaviour, a Drucker-Prager
221 material model with assumption of soil in elastic-perfectly plastic behavior and follows
222 an associated flow rule (dilatancy angle ψ equal to friction angle ϕ) was used with
223 material parameters of $\beta = 44.5$ and $d = 135$. Terms β and d represent parameters of the
224 material model which can be calculated indirectly using parameters of the Mohr-
225 Coulomb model derived from Ciampi [36].

226 The ‘Small Sliding’ contact in ABAQUS was used to simulate the interaction between
227 the soil and the buckets/mats. This type of interaction is used to simulate contact
228 between two deformable bodies or a deformable body and a rigid body in 3D. The soil
229 and the bucket were modelled using the C3D8R solid homogeneous elements available
230 in the ABAQUS element library, which are 8-noded linear brick elements with reduced
231 integration and hourglass control (an option for reduced-integration elements
232 in ABAQUS/Standard). The interaction between the sand and the caissons was modeled
233 by defining tangential and normal contact behavior in the FE model. Normal interaction
234 between mat-soil was simulated by a “hard” contact. Allowed separation after contact
235 was also used for interfaces of soil-caisson and mat-soil.

236

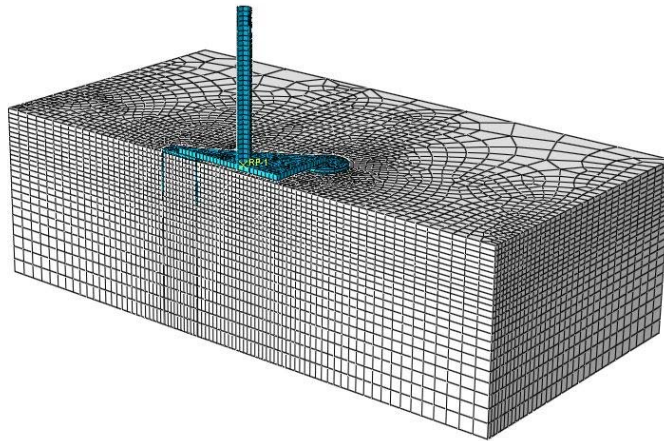
237 Fig. 6 shows a half model cutting through a diametrical plane of the tripod
238 hybrid bucket foundation with $L/D = 1$. The mesh dimensions were varied depending
239 on the bucket diameter and spacing. A relatively fine mesh was used around the bucket
240 and the mats, and becoming coarser further away from the bucket. In the FE analyses,
241 the foundations were modelled as “wished in place”, assuming that installation effects
242 had a negligible impact on the bearing capacity. The initial soil condition prior to

243 loading of the model foundation was generated considering a lateral earth pressure
244 coefficient $K_0 = 1 - \sin \phi$ [37].

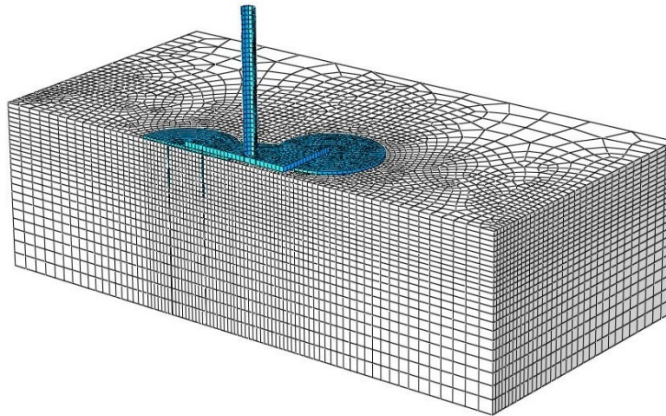
245 To simulate the overturning behaviour of the tripod foundation, a load-
246 controlled FE model was created. A 'Contact pair' interface was used to capture the
247 nonlinear behaviour of the soil-bucket interaction. The bucket outer surface was chosen
248 as the 'master surface' and the soil surface in contact with the skirt of the bucket as the
249 'slave surface'. The frictional force between these surfaces is dependent on a coefficient
250 of friction ?? [38]. In the numerical simulations presented here the friction coefficient
251 was calculated using $\tan(\delta)$, where δ is interface friction angle and assumed to be $2/3\phi$
252 [39]. The mats and the buckets were considered as linear elastic materials ($E=200$ GPa)
253 [40]. Elasticity modulus of sand is also calculated based on the formula proposed by
254 Seed and Idriss [41] and considered approximately 8000 kPa for the sand with relative
255 density of 23%.

$$G_{max} = 765.8(Dr)^{2/3}P_a\left(\frac{\sigma'_m}{P_a}\right)^{0.5}$$

256 Where σ'_m is mean principal effective stress, and P_a is the atmospheric pressure in the
257 same units as σ'_m .



258
259 (a)



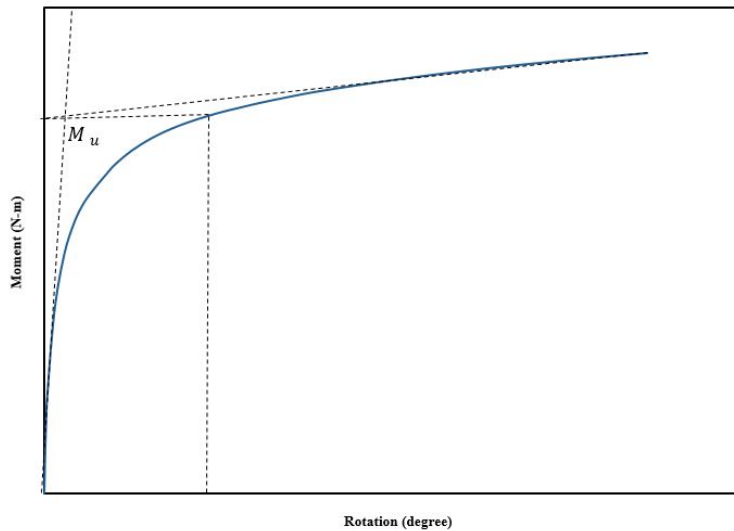
260

261 (b)

262 **Fig. 6.** Finite element model of the a) conventional and b) hybrid tripod bucket foundations used
263 to analyse the laterally loading behaviour

264

265 Based on the results of the FE analyses, the moment-rotation curves ($M - \theta$) of
266 the foundations were constructed to obtain the ultimate overturning capacity. The
267 curves are inherently nonlinear being controlled by the “elastic” stiffness at small
268 rotations and the moment capacity of the foundation at larger rotations. The ultimate
269 moment capacity of the foundation has been defined as the moment corresponding to
270 the yield point. To define the yield point, the method described by Villalobos [32] was
271 used. In this method, straight lines were fitted to the initial stiff elastic section and the
272 plastic section, as shown in Fig. 7. A horizontal line is then drawn from the intersection
273 point of the two fitted lines to the load-rotation angle curve. This line will be extended
274 until it cuts the moment-rotation curve, the intersection between the horizontal line and
275 the curve was defined as the ultimate moment, denoted as M_u .



276

277 **Fig. 7.** Tangent intersection method for determining the yield point and hence the ultimate
 278 bearing capacity of the foundation (M_u)

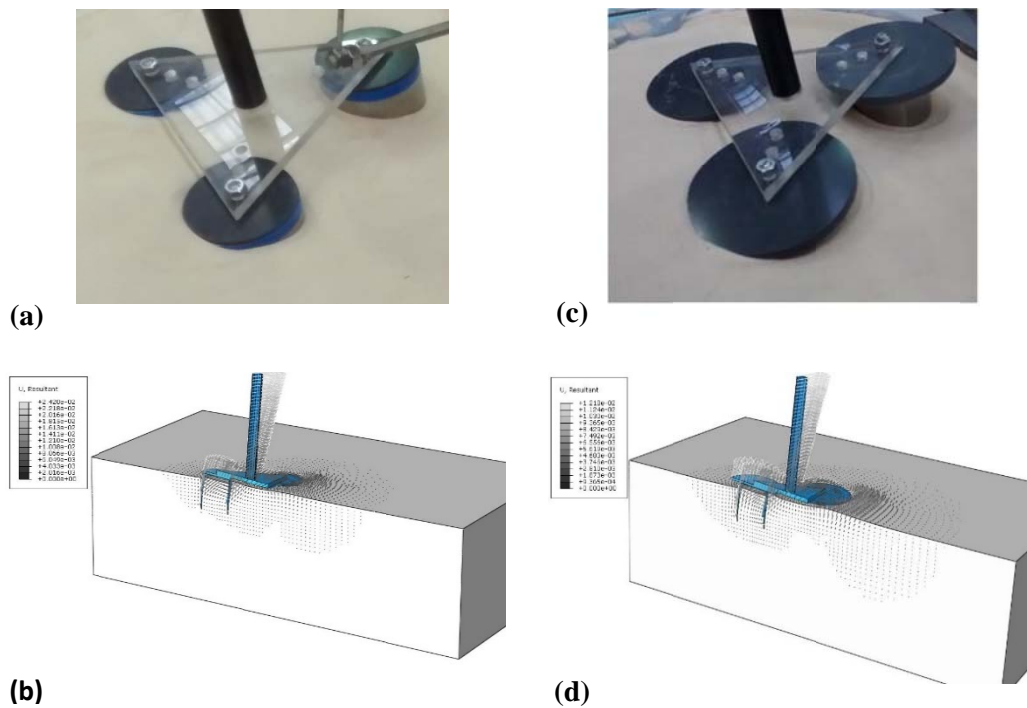
279

280 **5. Results and Analysis**

281 The experiments using the convention foundations in the C1-C6 series (as listed
 282 in Table 2) were conducted under identical test conditions, including soil density,
 283 bucket aspect ratio ($L/D=1$) and type of loading, although bucket spacing (S) was
 284 varied from 90 mm to 165mm (see Table 2). The experiments H1-H4 were carried out
 285 on the hybrid tripod bucket foundations with circular mats of diameter 1.6 times larger
 286 than the bucket diameter ($D'=120$ mm) in the same sequence and under the same
 287 experimental conditions as the C1-C6 experiments. The remaining models in Table 2
 288 (i.e. C7-C10, and H5-H14) refer to FE models that were created to identify the effect of
 289 different spacing and different mat size beyond those used in the experiments. All the
 290 experiments assigned odd numbers within the test IDs (e.g. C1, C3, H1, H3) are for
 291 models subjected to a forward loading direction, while the even numbers (e.g. C2, C4,
 292 H2, H4) are for the models loaded in the backward direction.

293 The tripod foundation resists the overturning moment with the reaction generated in the
 294 windward and leeward bucket foundations acting in tension and compression,
 295 respectively [42, 43]. Based on the deformation mechanisms, observed in Fig. 8, the

296 overturning moment is resisted by a combination of tension and compression on the
297 windward and leeward in both conventional and hybrid tripod foundations.



298
299 **Fig. 8.** Failure mechanism due to an overturning moment in the forward direction, (a)
300 EXP conventional foundation, (b) FEM conventional foundation, (c) EXP hybrid foundation, (d)
301 FEM hybrid foundation

302
303
304

305 **5.1 The effect of bucket spacing and loading direction on the capacity of** 306 **conventional foundation (Finite Element and Experimental Modelling)**

307 Initially, the impact of the bucket spacing on the overturning moment capacity of the
308 conventional and hybrid tripod bucket foundations are examined. The experiments were
309 performed by applying a monotonic horizontal load at the top of the tower, with an
310 eccentricity from the top of the foundations ($e = 230$ mm). This load was applied until
311 failure was reached. The numerical and experimental results have been compared based
312 on the direction of the load and bucket spacing of both the conventional and hybrid

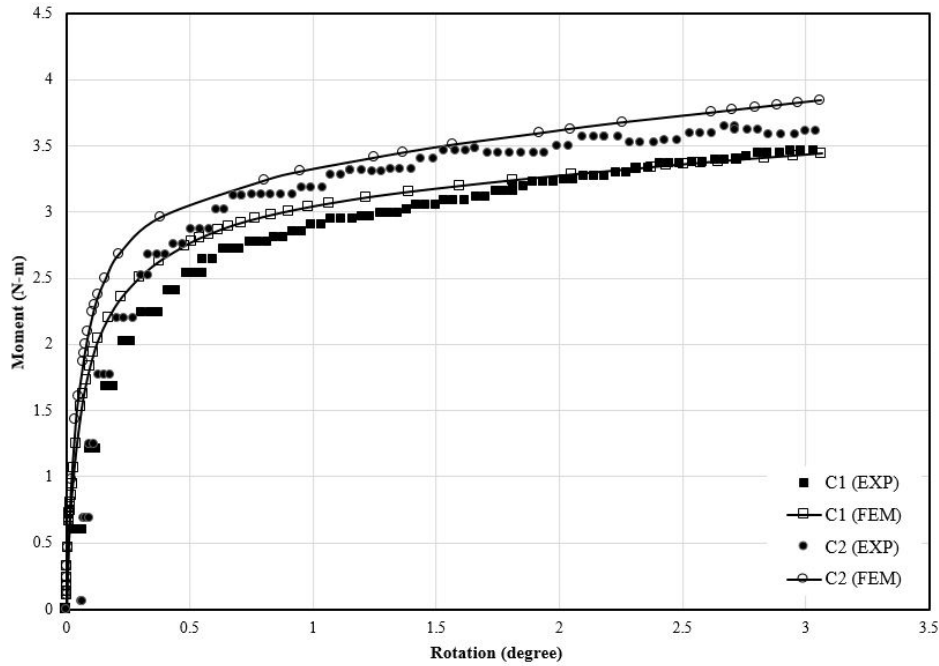
313 tripod foundations. The comparison demonstrated that the numerical simulations
314 provide very close results (<10% average error) to the experimental data (Figs. 9-13).
315 As can be seen in Figures 9-13, the bearing capacity of the conventional tripod due to
316 an overturning moment is higher when the foundations are subjected to the backward
317 loading direction, i.e. the foundation with $S=95$ mm maintained an almost 18% higher
318 capacity under backward loading compared with the experiments loaded in the forward
319 direction (Fig. 9).

320 The horizontal resistance of a tripod depends on the loading direction due to the
321 asymmetry of the foundations [44]. Previous studies have revealed that the capacity of
322 tripod systems is primarily governed by the pull-out capacity of the windward bucket
323 [43, 44]. It should also be noted, however, that the capacity of single suction buckets
324 under pull-out is lower than in compression [45]. Hence, the number of windward
325 buckets in the tripod foundation could control the overall capacity. Accordingly, the
326 two windward buckets provide a higher capacity compared with the scenario where two
327 buckets are in compression. Therefore, the most critical loading condition for tripods is
328 when the horizontal loading is imposed in the forward direction (F), i.e. where one
329 bucket of the tripod resists pull-out load, as shown in Fig. 8. This observation for
330 conventional tripod foundations is similar to that reported by Kim et al. [44].

331

332

333



334

335 **Fig. 9.** Moment-rotation plot for the conventional foundation system with a spacing dimension
 336 of 95 mm (EXP and FEM)

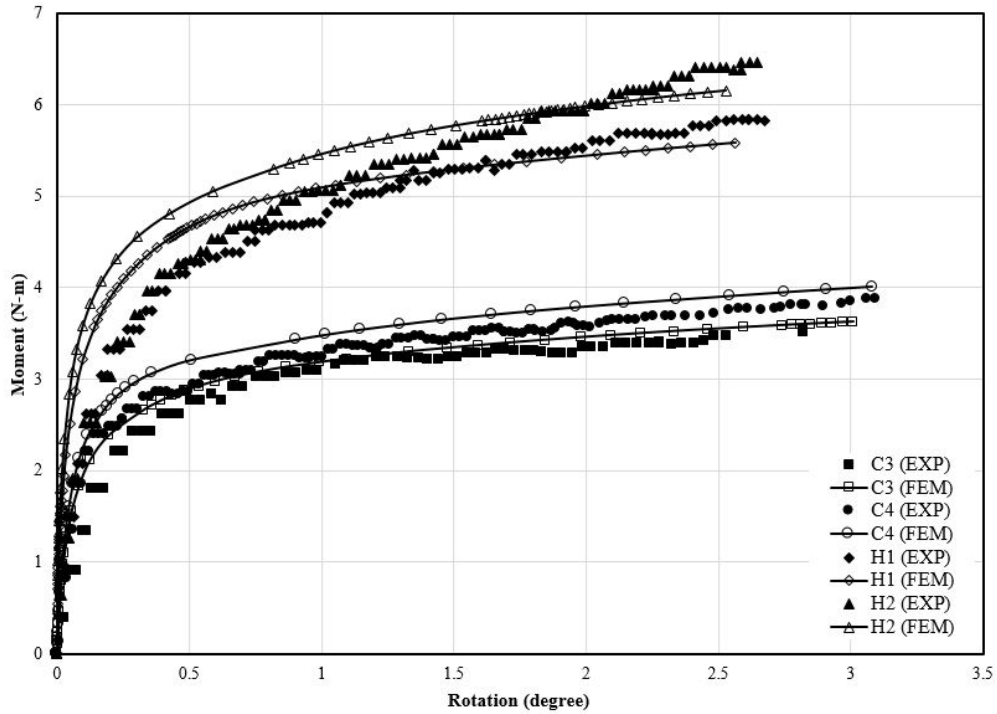
337

338 **5.2 The effect of the hybrid system on the capacity improvement of tripod**
 339 **bucket foundations**

340 The impact of using a hybrid system on the overturning capacity of a tripod bucket
 341 foundation is presented by means of a series of laboratory tests and numerical
 342 modelling. Comparing Figs. 10 and 11, it is clear that there is a significant increase in
 343 the overturning capacity provided by the hybrid tripod foundation. The test results show
 344 that the overturning capacity of the tripod bucket foundation, under the forward loading
 345 direction, was increased by approximately 47% and 45%, for bucket spacings of 130
 346 mm and 165 mm, respectively (Figs. 10 and 11). For the same spacing, the ultimate
 347 overturning bearing capacity increased by approximately 43% and 38%, for the models
 348 under the backward loading direction.

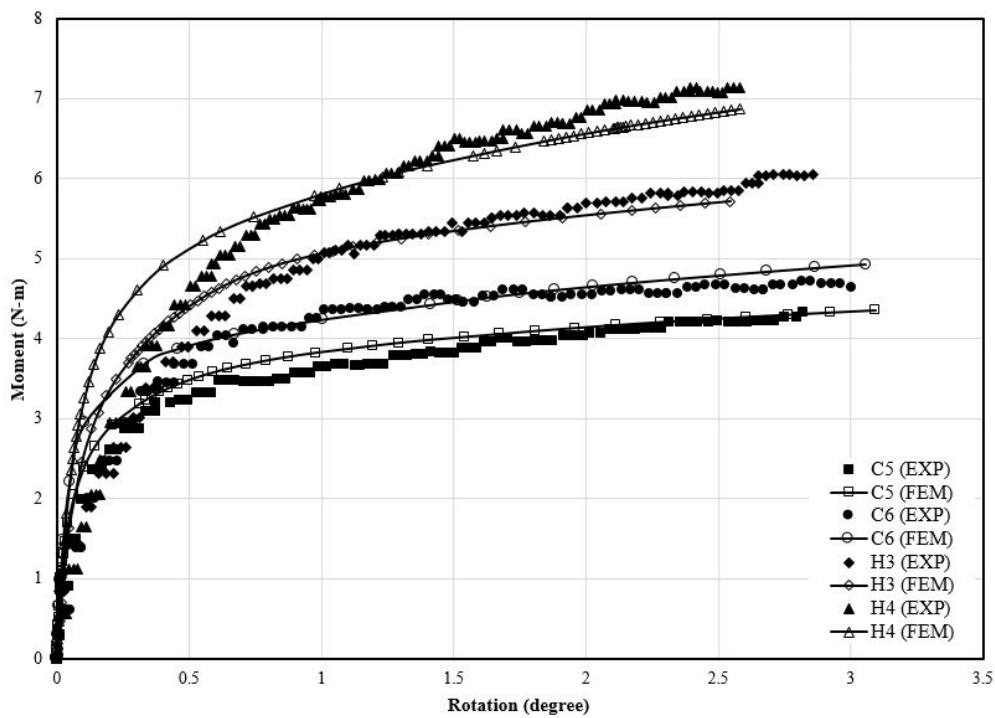
349 Based on the results, it is evident that attaching circular mats can provide additional
 350 resistance compared to the original tripod foundation. The contact surfaces between the
 351 circular mats and the seabed and the development of bearing stress beneath the mats
 352 provides a larger restoring moment to withstand the rotation. Moreover, the circular

353 mats induce additional vertical stresses in the soil beneath the foundation, thereby
354 helping to increase the shear resistance of the soil and further resisting rotation.
355



356
357 **Fig. 10.** Moment-rotation plot for conventional and hybrid foundation systems with a bucket
358 spacing of 130 mm (EXP and FEM)

359



360

361 **Fig. 11.** Moment-rotation plot for conventional and hybrid foundation systems with a bucket
362 spacing of 165 mm (EXP and FEM)

363

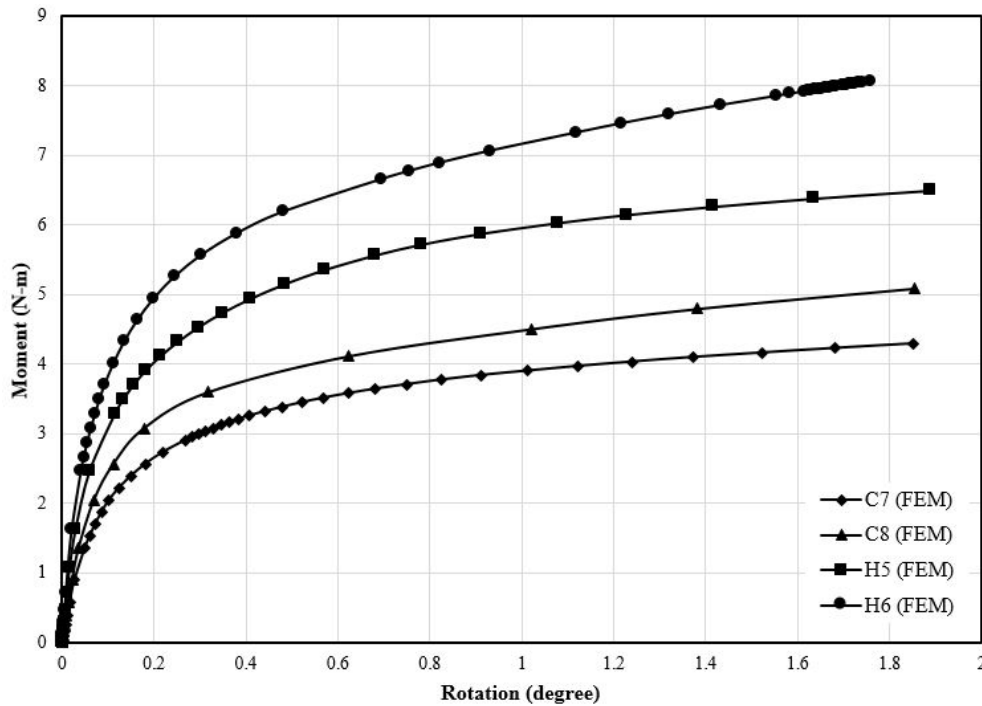
364 **5.3 The effect of bucket spacing size and mat diameter on the improvement of** 365 **capacity of hybrid system (FEM)**

366 The results from the three-dimensional finite element analyses (FEM) for the
367 two tripod foundation models (with and without circular mats) are presented in Figs.
368 12-14 in terms of the moment and rotation with varying circular mat diameters and
369 bucket spacing.

370 A series of numerical models (C7, C8, H5 and H6) were performed in which
371 the mat diameter was kept the same as those used in the previous models ($D' =$
372 120 mm) while the bucket spacing was changed to $S = 200\text{ mm}$ in order to evaluate
373 the effect of higher spacing on the overturning moment resistance of the conventional
374 and hybrid tripod foundations.

375 The moment-rotation ($M - \theta$) curves for the conventional and hybrid tripod
376 models with diameter $D' = 120\text{ mm}$ and spacing $S = 200\text{ mm}$ installed in loose sand
377 with relative density of $Dr = 23\%$ are presented in Fig. 12. The results from the FEM
378 indicated that the mats used in the proposed foundation have a significant impact on
379 improving the overturning capacity. The mat aids the resisting force against the external
380 load by extending the contact area. The results also showed that the overturning
381 capacity of the tripod bucket foundation was increased by approximately 53%, and 47%
382 for the hybrid bucket foundation, under F and B load conditions.

383



384

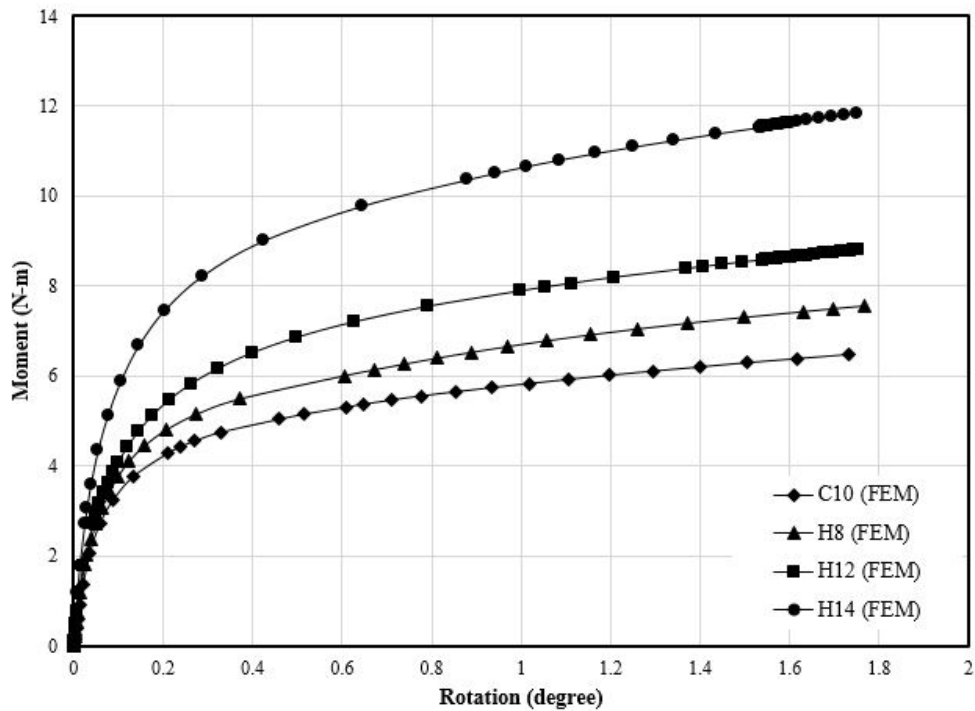
385 **Fig. 12.** Comparison of the moment-rotation plots for conventional and hybrid foundations with
 386 a bucket spacing of 200 mm (FEM)

387

388 A FEM was also developed to investigate the effects of the mat diameter to
 389 improve the capacity of the hybrid tripod bucket foundations. The models C9, C10, H7,
 390 H8, H11, H12, H13 and H14 were selected with mat sizes both smaller and larger than
 391 those used in the reference models ($D' = 120\text{ mm}$). When $\frac{S}{D}$ equals 3.13, the ultimate
 392 overturning bearing capacity increased by approximately 18%, 36% and 80% for hybrid
 393 tripod models under a backward loading system with mat diameter ratios ($\frac{D'}{D}$) equal to
 394 1.3, 1.9 and 2.4, respectively (see Fig. 13). However, it is worth noting that combining
 395 circular mats with the buckets results in a slightly better overturning capacity under
 396 forward loading compared with backward loading. When $\frac{S}{D}$ equals 3.13, the ultimate
 397 overturning capacity increased by approximately 25%, 50%, and 100% for hybrid
 398 tripod models with mat diameter ratios ($\frac{D'}{D}$) of approximately 1.3, 1.9, and 2.4,
 399 respectively (Fig.14). Given the most unstable loading scenario is when the horizontal
 400 loading is imposed in the forward direction (F) [44], two circular mats attached to the

401 two buckets at the leeward side provides higher resistance against overturning
402 moments. This resistance corresponds to the larger contact surface areas between the
403 circular mats, attached to the leeward buckets, and the seabed during the loading. In the
404 forward direction, only the mat attached to the bucket at the leeward resists the
405 horizontal load because the two other mats on the windward side are lifted from the soil
406 surface when the whole foundation is rotating.

407

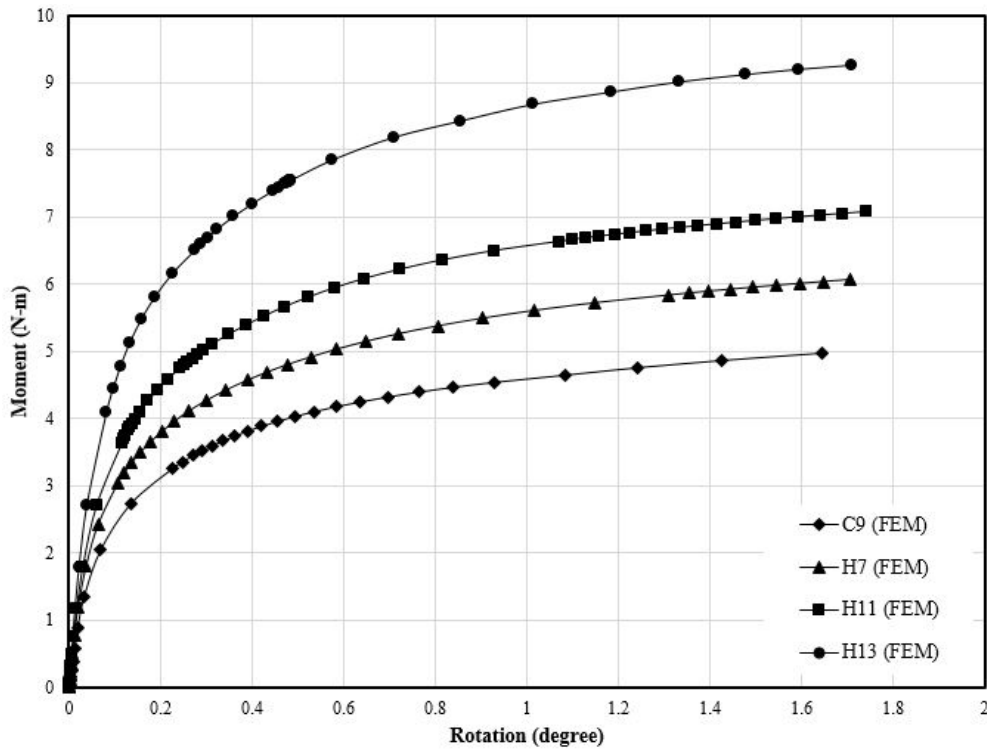


408

409 **Fig. 13.** Comparison of the moment-rotation plots for conventional and hybrid foundations with
410 a bucket spacing of 235 mm and varying circular mat sizes, due to a backward loading direction
411 (FEM)

412

413



414

415 **Fig. 14.** Comparison of the moment-rotation plots for conventional and hybrid foundations with
 416 a bucket spacing of 235 mm and varying circular mat sizes, due to a forward loading direction
 417 (FEM)

418

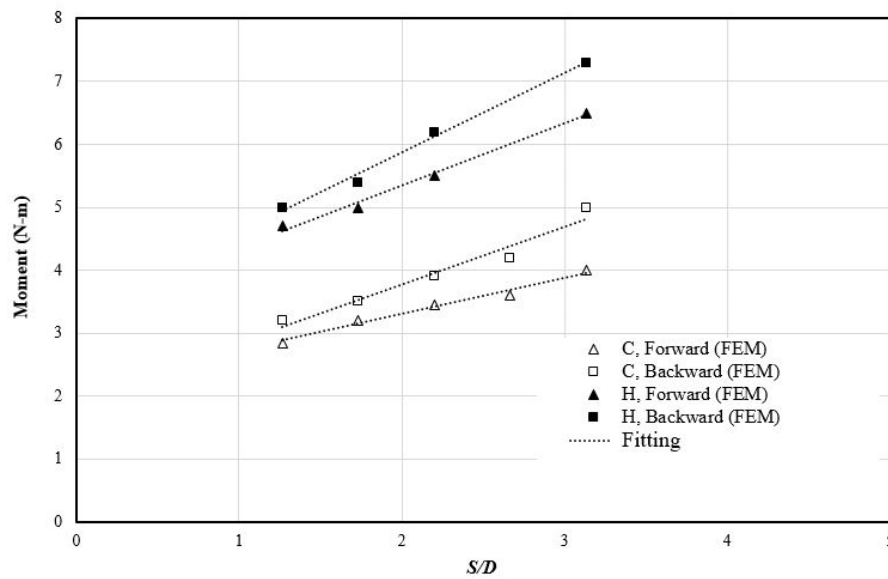
419

420 Fig. 15 illustrates the variation in M_u with the normalized footing spacing S/D
 421 for the conventional and hybrid tripod foundations under the forward and backward
 422 loading directions. The hybrid models are enhanced with the circular mat diameter of
 423 120 mm. As expected, M_u increases significantly as S/D increases, which is due to the
 424 increase in the lever arm length with an increase in S/D . The bearing capacity of tripod
 425 bucket foundations is influenced by the spacing between the buckets because of their
 426 mutual interaction [21].

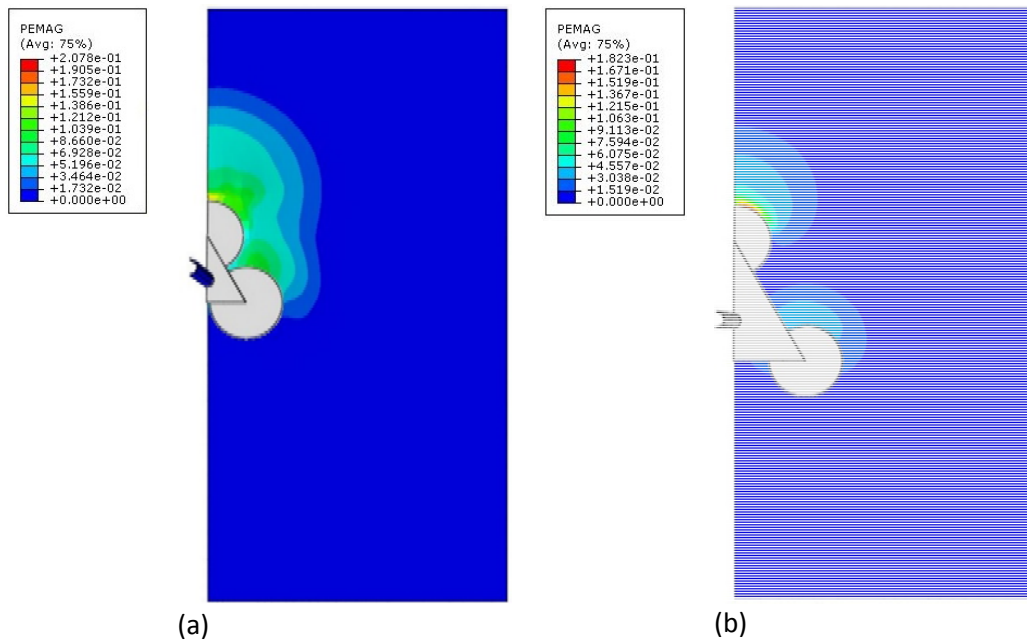
427 In general, the interactions in a hybrid tripod bucket foundation can be
 428 classified into two categories: the interaction between buckets (bucket–soil–bucket) and
 429 the interaction between mat and bucket (mat–soil–bucket). A close spacing between
 430 individual caissons in a tripod caisson results in overlapping stress zones.

431 Due to the larger surface area between the soil and the circular mats in the
 432 hybrid foundation, relatively large stress zones occur along the contact interface when
 433 the foundation system is subjected to an overturning moment. For hybrid tripod
 434 foundations, the overlap of the stress zones are even larger due to the presence of the
 435 mats. The intensity of the stresses will be affected by the centre-to-centre spacing of the
 436 buckets (Fig. 16). In ABAQUS, PEMAG refers to the plastic strain magnitude.

437 Therefore, it can be concluded that the divergences in Fig. 15 are due to the
 438 different overlapping stress zones, which can influence the capacity of the foundations.
 439



440
 441 **Fig. 15.** Variation of M_u with S/D for loading directions F and B (FEM)
 442



443

444 **Fig. 16.** Plan view of the shear zone formation in hybrid tripod foundations from the FEM
 445 results, (a) H2, (b) H10.

446

447 **5.4 Large-Scale Numerical Modelling**

448 **5.4.1 Validation of finite element modelling against large-scale field trials**

449 To understand the large-scale behaviour of the proposed tripod foundation, a series of
 450 FE models were developed to study their behaviour in field conditions. Initially,
 451 validation against two large-scale field trials on single suction caisson foundations
 452 available from literature were carried out to ensure the accuracy of our FE modelling.
 453 The FE models were then developed to predict the overturning capacity of the
 454 conventional and hybrid tripod foundations.

455 Of the available data in literature, two field tests were chosen to validate our FE
 456 models. The field tests were originally reported by Housby and Byrne [46] and
 457 Housby et al. [4] at the Sandy Haven and Frederikshavn test sites, respectively. The
 458 parameters used in the FEM simulations are given in Table 3. Both sites comprised of
 459 predominantly sandy soil. In the FE, the loading was simulated as drained to replicate
 460 the site condition.

461 The suction caisson at the Sandy Haven site had a diameter of 4 m and a skirt
462 length of 2.5 m, and it was installed in medium to dense sand. The foundation was
463 subjected to a constant vertical load of 100 kN. The horizontal load test was then
464 conducted at a loading point height of 14.5 m above the ground surface. The suction
465 caisson tested at the Frederikshavn site, which had a diameter of 2 m and a skirt length
466 of 2 m, was installed in dense sand. The foundation was subjected to horizontal loading
467 at a height of 17.4 m above the ground surface under a constant vertical load of 37.3
468 kN. Figures 17a, and 17b show that load-displacement curves obtained from the FE
469 analysis agreed well with those measured in the field tests and the centrifuge test. In the
470 numerical simulations presented here the friction coefficient was calculated using
471 $\tan(\delta)$, where δ is interface friction angle and assumed with the well-known
472 assumption of $\delta=2/3\phi$ [47]. The elastic modulus of the sands (E) is estimated based on
473 the shear modulus G proposed by Seed and Idriss [41]. An average penetration depth
474 was considered for estimation of equivalent modulus of elasticity. The modulus of
475 elasticity(E), 210GPa and Poisson's ratio (ν), 0.3 were used as the steel properties [48].

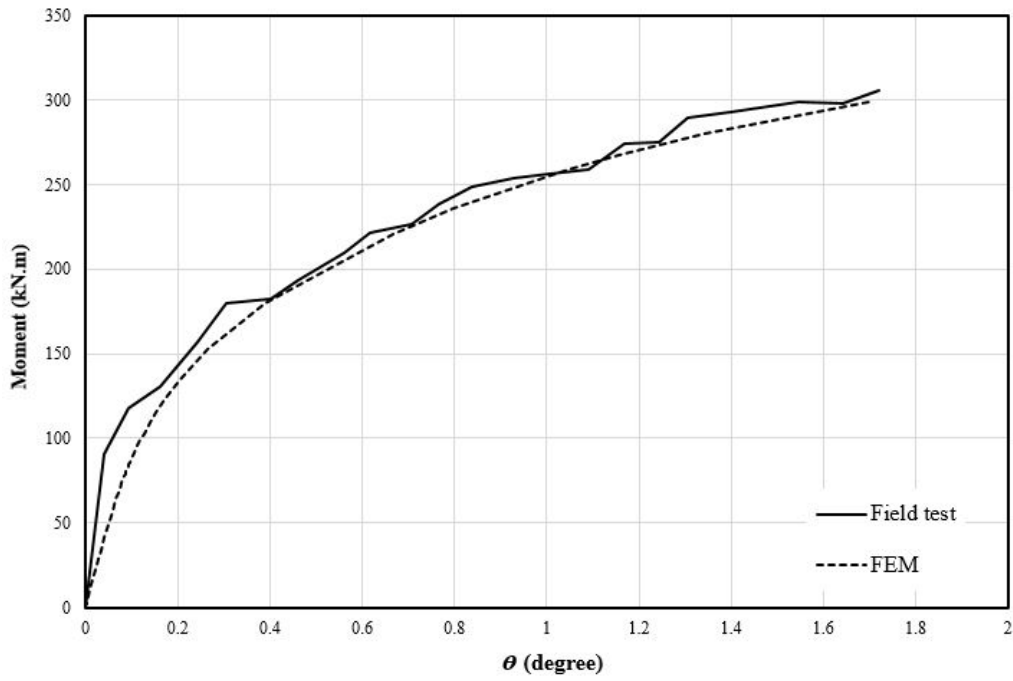
476

477 **TABLE 3.** Detailed reference studies for validation of FEM modelling

| Case study | Diameter (D) | Length (L) | Load eccentricity (e) | Aspect ratio (L/D) | Effective unit weight (γ') | Internal friction angle (ϕ) |
|--------------------|---------------------|-------------------|---------------------------------|------------------------------|---|--|
| Frederikshavn [46] | 2m | 2m | 17.4m | 1 | 9 | 37-38 |
| Sandy Haven [4] | 4m | 2.5m | 14.5m | 0.625 | 8.5 | 34 |

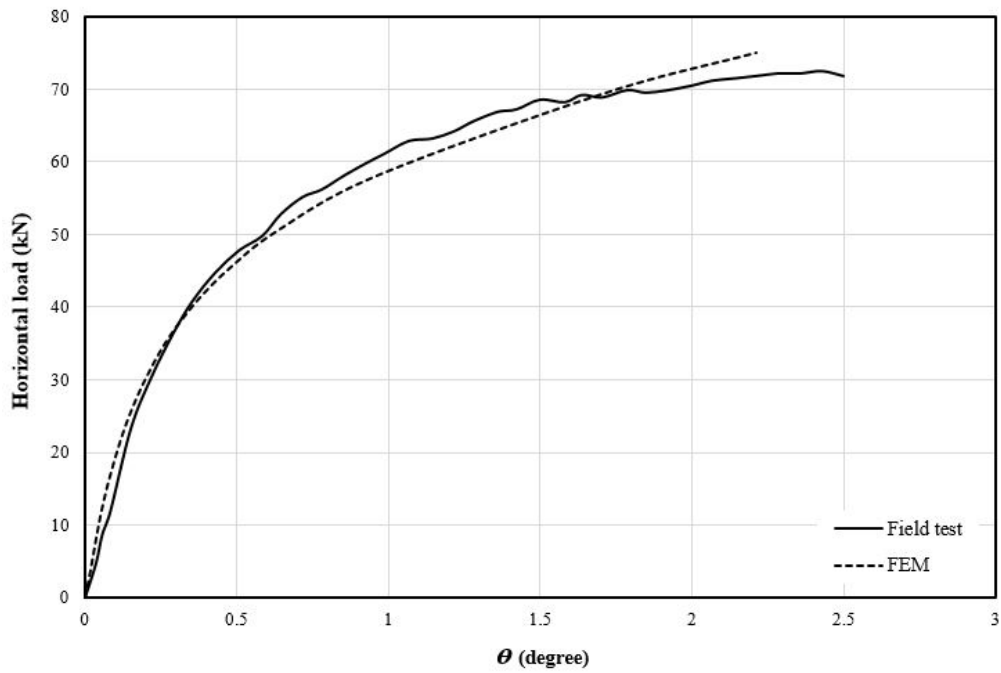
478

479



480

481 (a)



482

483 (b)

484 **Fig. 17.** Comparison of the numerical modelling and the field test results a) Frederikshavn, b)
485 Sandy haven

486

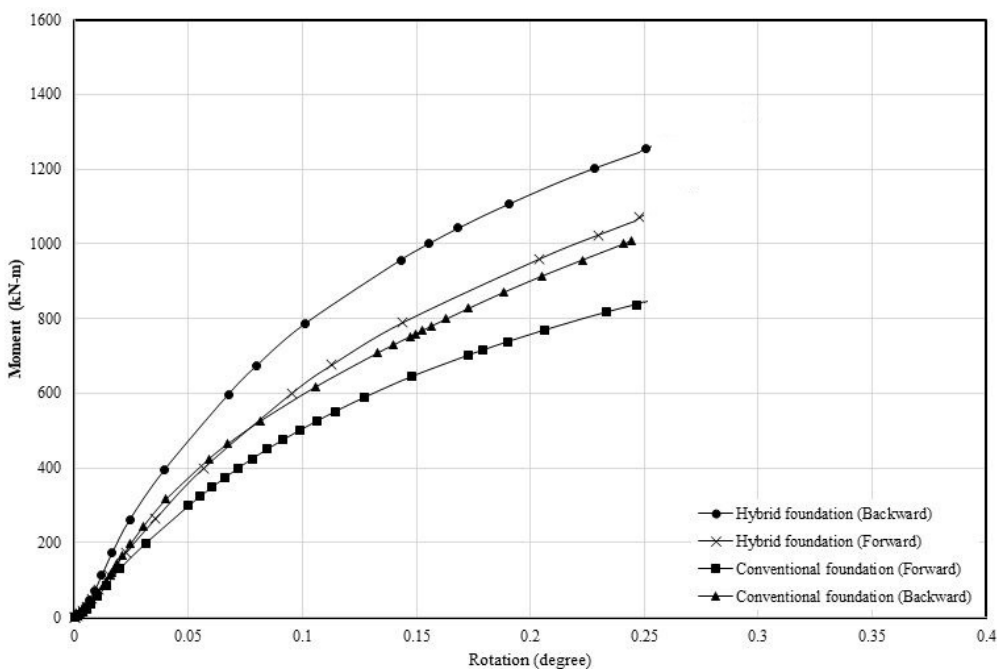
487

488 **5.4.2 FE modelling of large-scale hybrid tripod foundation**

489 The validated FE model was subsequently used to predict the overturning
 490 capacity of a hypothetical full-size tripod foundation ($L/D = 1$), with three caissons of
 491 diameter 2 m, circular mats of diameter 1.9 times larger than the bucket diameter
 492 ($D'=3.8$ m) and spacing $S = 6.3$ m under a constant vertical load of 37.3 kN. The soil
 493 parameters and loading condition were adopted from Housby et al. [49]. Conventional
 494 and hybrid tripod foundations were modelled and the improvement in overturning
 495 moment under forward and backward loading conditions were recorded. Assume the
 496 maximum allowable tilting angle of the foundation must be smaller than 0.25 degree
 497 [50, 51]. Accordingly, for the given foundations the results are presented in terms of
 498 maximum allowable tile at foundation head (Fig. 18).

499 Based on the results from numerical analysis, the allowable overturning bearing
 500 capacity for the foundation with mat diameter ratios ($\frac{D'}{D}$) equal to 1.9, increased by
 501 approximately 27%, and 30% under a forward and backward loading systems,
 502 respectively (see Fig. 18).

503



504

505 **Fig. 18.** Comparison of the moment-rotation plots for the conventional and hybrid foundations
506 with a bucket spacing of 6.3 m and circular mat size of 3.8 m, due to a forward and backward
507 loading direction (FEM)

508

509 It is clear from the experiments and the FEM studies that there are benefits of using
510 circular mats in combination with buckets to enhance the overall capacity of tripod
511 suction bucket foundations. Making an effort to reduce the high costs associated with
512 manufacturing and installing of a conventional tripod foundation (with large diameter)
513 at large spacing, the hybrid foundation can provide cost effective operation for offshore
514 wind turbines.

515 Since the main goal of this paper was to evaluate the bearing capacity improvement of
516 the proposed foundation, the structural aspects were beyond the scope of this study and
517 were not evaluated; however, the analysis must account for the structural behaviour of
518 the proposed foundation in the future design.

519 In the present study, drained conditions have been assumed for the experiments,
520 however the models should also be examined under partially drained or undrained
521 conditions. Tripod bucket foundations may be installed in a variety of soils, therefore
522 the effectiveness of mats for tripod bucket foundations installed in different soil types,
523 with different sand density, should also be investigated. Further studies are also
524 necessary in order to investigate the behaviour of the hybrid tripod bucket foundations
525 under combined loads.

526

527

528 **6. Conclusions**

529 In this study a novel hybrid tripod bucket foundation has been proposed with the
530 intention of improving the overturning capacity of bucket foundations typically
531 designed for offshore wind turbines. The behaviour of conventional and hybrid tripod
532 bucket foundations subjected to an overturning moment with different bucket spacings

533 and circular mat sizes has been investigated using 1g experimental studies and three-
534 dimensional nonlinear FEM analyses in loose dry sand (drained condition).

535 The results obtained from the experimental and numerical studies were compared to
536 validate the FEM and to assess the suitability and possible benefits of using hybrid
537 tripod bucket foundations. Based on the results, the following key conclusions can be
538 drawn:

- 539 • Tripod foundations combined with three circular mats provides considerably
540 higher overturning capacity compare with a conventional tripod foundation
541 (between 25–100% depending on the diameter of the circular mats and the
542 spacing of the buckets).
- 543 • The overturning capacity of the conventional and the hybrid tripod bucket
544 foundations is influenced by the loading direction, where higher capacity is
545 usually achieved under backward loading, i.e. where the loading direction is
546 towards a single bucket of a tripod foundation and the other two buckets are
547 being rotated out of the seabed.
- 548 • The overturning capacity of the conventional and the hybrid tripod bucket
549 foundations depends greatly on the centre-to-centre distance between the
550 buckets and the direction of the load. In general, the overturning capacity
551 increases as the bucket spacing increases.

552

553

554

555

556 **Reference:**

- 557 1. Randolph, M., et al. *Challenges of offshore geotechnical engineering*. in
558 *Proceedings of the international conference on soil mechanics and*
559 *geotechnical engineering*. 2005. AA Balkema Publishers.
- 560 2. Byrne, B., et al., *Suction caisson foundations for offshore wind turbines*. Wind
561 Engineering, 2002. **26**(3): p. 145-155.
- 562 3. Cox, J.A. and S.J.P.o.t.I.o.C.E.G.E. Bhattacharya, *Serviceability of suction caisson*
563 *founded offshore structures*. 2016. **170**(3): p. 273-284.

- 564 4. Houlsby, G.T., L.B. Ibsen, and B.W. Byrne, *Suction caissons for wind turbines*.
565 Frontiers in Offshore Geotechnics: ISFOG, Perth, WA, Australia, 2005: p. 75-93.
- 566 5. Cotter, O., *Installation of suction caisson foundations for offshore renewable*
567 *energy structures*. 2010, Oxford University.
- 568 6. Veritas, D.N., *Design of Offshore Wind Turbine Structure*. Offshore Standard
569 DNV-OS-J101, 2004.
- 570 7. Kim, S.-R. and M. Oh, *Group effect on bearing capacities of tripod bucket*
571 *foundations in undrained clay*. Ocean Engineering, 2014. **79**: p. 1-9.
- 572 8. Villalobos, F.A., G.T. Houlsby, and B.W. Byrne. *Suction caisson foundations for*
573 *offshore wind turbines*. in *Proc. 5th Chilean Conference of Geotechnics*
574 *(Congreso Chileno de Geotecnia)*, Santiago. 2004.
- 575 9. Sukumaran, B., et al., *Efficient finite element techniques for limit analysis of*
576 *suction caissons under lateral loads*. Computers and Geotechnics, 1999. **24**(2):
577 p. 89-107.
- 578 10. Bakmar, C.L., et al. *The Monopod Bucket Foundation: recent experiences and*
579 *challenges ahead*. in *The European Offshore Wind Conference & Exhibition*.
580 2009. European Offshore Wind Conference 2009.
- 581 11. Welschen, Y., *Suction bucket buckling: Buckling behaviour of suction buckets*
582 *during installation in layered soils*. 2015.
- 583 12. Bienen, B., et al., *Numerical modelling of a hybrid skirted foundation under*
584 *combined loading*. Computers and Geotechnics, 2012. **45**: p. 127-139.
- 585 13. CIVILE, C.D.L.I.I., *Behaviour of Monopod Bucket Foundations Under Horizontal*
586 *Load in Dense Sand*. 2011.
- 587 14. Harireche, O., M. Mehravar, and A.M. Alani, *Soil conditions and bounds to*
588 *suction during the installation of caisson foundations in sand*. Ocean
589 Engineering, 2014. **88**: p. 164-173.
- 590 15. Mehravar, M., O. Harireche, and A. Faramarzi, *Evaluation of undrained failure*
591 *envelopes of caisson foundations under combined loading*. Applied Ocean
592 Research, 2016. **59**: p. 129-137.
- 593 16. Faramarzi, A., et al., *MODELLING THE SEEPAGE FLOW DURING CAISSON*
594 *INSTALLATION IN A NATURAL SEABED*. Proceedings of the 24th UK Conference
595 of the Association for Computational Mechanics in Engineering, 2016(Cardiff
596 University, Cardiff.): p. 150-153.
- 597 17. Houlsby, G. and B. Byrne, *Calculation procedures for installation of suction*
598 *caissons*. Report No. OUEL2268/04, University of Oxford, 2004.
- 599 18. Achmus, M., C. Akdag, and K. Thieken, *Load-bearing behavior of suction bucket*
600 *foundations in sand*. Applied Ocean Research, 2013. **43**: p. 157-165.
- 601 19. Kim, S.R., *Evaluation of vertical and horizontal bearing capacities of bucket*
602 *foundations in clay*. Ocean Engineering, 2012. **52**: p. 75-82.
- 603 20. Zhu, B., et al., *Deflection-based bearing capacity of suction caisson foundations*
604 *of offshore wind turbines*. Journal of Geotechnical and Geoenvironmental
605 Engineering, 2014. **140**(5): p. 04014013.
- 606 21. Tran, N.X. and S.-R. Kim, *Evaluation of horizontal and moment bearing*
607 *capacities of tripod bucket foundations in sand*. Ocean Engineering, 2017. **140**:
608 p. 209-221.
- 609 22. Kim, S.-R., *Evaluation of combined horizontal-moment bearing capacities of*
610 *tripod bucket foundations in undrained clay*. Ocean Engineering, 2014. **85**: p.
611 100-109.
- 612 23. Gourvenec, S. and K. Jensen, *Effect of embedment and spacing of cojoined*
613 *skirted foundation systems on undrained limit states under general loading*.
614 International Journal of Geomechanics, 2009. **9**(6): p. 267-279.

615 24. Stergiou, T., D. Terzis, and K. Georgiadis, *Undrained bearing capacity of tripod*
616 *skirted foundations under eccentric loading*. *geotechnik*, 2015. **38**(1): p. 17-27.

617 25. Kim, D.-J., et al. *Numerical Analysis of Cluster and Monopod Suction Bucket*
618 *Foundation*. in *ASME 2013 32nd International Conference on Ocean, Offshore*
619 *and Arctic Engineering*. 2013. American Society of Mechanical Engineers.

620 26. Kim, J.H., et al., *Bearing capacity of hybrid suction foundation on sand with*
621 *loading direction via centrifuge model test*. Japanese Geotechnical Society
622 Special Publication, 2016. **2**(37): p. 1339-1342.

623 27. Gaudin, C., et al. *Centrifuge experiments of a hybrid foundation under*
624 *combined loading*. in *The Twenty-first International Offshore and Polar*
625 *Engineering Conference*. 2011. International Society of Offshore and Polar
626 Engineers.

627 28. Fu, D., et al., *Undrained capacity of a hybrid subsea skirted mat with caissons*
628 *under combined loading*. *Canadian Geotechnical Journal*, 2014. **51**(8): p. 934-
629 949.

630 29. Wang, X., et al., *Lateral bearing capacity of hybrid monopile-friction wheel*
631 *foundation for offshore wind turbines by centrifuge modelling*. *Ocean*
632 *Engineering*, 2018. **148**: p. 182-192.

633 30. Arshi, H. and K. Stone. *Lateral Resistance of Hybrid Monopile-Footing*
634 *Foundations In Cohesionless Soils For Offshore Wind Turbines*. in *Offshore Site*
635 *Investigation and Geotechnics: Integrated Technologies-Present and Future*.
636 2012. Society of Underwater Technology.

637 31. Wang, X., et al., *A review on recent advancements of substructures for offshore*
638 *wind turbines*. *Energy Conversion and Management*, 2018. **158**: p. 103-119.

639 32. Villalobos J, F., *Model testing of foundations for offshore wind turbines*. 2006,
640 University of Oxford.

641 33. Kelly, R., et al. *Tensile loading of model caisson foundations for structures on*
642 *sand*. in *The Fourteenth International Offshore and Polar Engineering*
643 *Conference*. 2004. International Society of Offshore and Polar Engineers.

644 34. Villalobos, F.A., B.W. Byrne, and G.T. Housby. *Moment loading of caissons*
645 *installed in saturated sand*. in *Proceedings of international symposium on*
646 *frontiers in Geotechnics, ISFOG*. University of Western. 2005.

647 35. Villalobos Jara, F.A., *Model testing of foundations for offshore wind turbines*.
648 2006, University of Oxford.

649 36. Ciampi, V., *MA Crisfield, Non-linear Finite Element Analysis of Solids and*
650 *Structures*. *Meccanica*, 1997. **32**(6): p. 586-587.

651 37. Jaky, I., *The coefficient of earth pressure at rest*. *Journal Soc. of Hungarian*
652 *Architects and Engineers*, 1944: p. 355-358.

653 38. Abdel-Rahman, K. and M. Achmus. *Behavior of foundation piles for offshore*
654 *wind energy plants under axial cyclic loading*. in *Proceedings of Simulia*
655 *Customer Conference*. 2011.

656 39. Ahmed, S.S., B. Hawlader, and K. Roy. *Finite Element Modeling of Large*
657 *Diameter Monopiles in Dense Sand for Offshore Wind Turbine Foundations*. in
658 *ASME 2015 34th International Conference on Ocean, Offshore and Arctic*
659 *Engineering*. 2015. American Society of Mechanical Engineers.

660 40. Abdelkader, A.M.R., *Investigation of Hybrid Foundation System for Offshore*
661 *Wind Turbine*. 2015.

662 41. Seed, H.B.a.I., I.M. , *Soil moduli and damping factors for dynamic response*
663 *analysis*. Report No. UCB/EERC-70/10. University of California, Berkeley, 1970.

- 664 42. Byrne, B. and G. Houlsby, *Foundations for offshore wind turbines*. Philosophical
665 Transactions: Mathematical, Physical and Engineering Sciences, 2003: p. 2909-
666 2930.
- 667 43. Senders, M., *Suction caissons in sand as tripod foundations for offshore wind*
668 *turbines*. 2009: University of Western Australia.
- 669 44. Kim, D.-J., et al., *Investigation of monotonic and cyclic behavior of tripod*
670 *suction bucket foundations for offshore wind towers using centrifuge*
671 *modeling*. Journal of Geotechnical and Geoenvironmental Engineering, 2014.
672 **140**(5): p. 04014008.
- 673 45. Nabipour, M. and H. Matin Nikoo, *An Investigation into the Pull-out Failure*
674 *Mechanisms of Suction Caissons*. International Journal of Maritime
675 Technology, 2015. **4**: p. 21-35.
- 676 46. Houlsby, G.T. and B.W. Byrne, *Suction caisson foundations for offshore wind*
677 *turbines and anemometer masts*. Wind engineering, 2000. **24**(4): p. 249-255.
- 678 47. Foglia, A., M. Kohlmeier, and M. Wefer, *Physical modeling and numerical*
679 *analyses of vibro-driven piles with evaluation of their applicability for offshore*
680 *wind turbine support structures*. Proc nord geotech meet, 2016.
- 681 48. Bagheri, P., S.W. Son, and J.M. Kim, *Investigation of the load-bearing capacity*
682 *of suction caissons used for offshore wind turbines*. Applied Ocean Research,
683 2017. **67**: p. 148-161.
- 684 49. Houlsby, G.T. and B.W. Byrne, *Design procedures for installation of suction*
685 *caissons in clay and other materials*. Proceedings of the Institution of Civil
686 Engineers-Geotechnical Engineering, 2005. **158**(2): p. 75-82.
- 687 50. Bhattacharya, S., *Challenges in design of foundations for offshore wind*
688 *turbines*. Engineering & Technology Reference, 2014. **1**(1): p. 1-9.
- 689 51. Wang, L., et al., *Comparison of monotonic and cyclic lateral response between*
690 *monopod and tripod bucket foundations in medium dense sand*. Ocean
691 Engineering, 2018. **155**: p. 88-105.

692

693